J. Fluid Mech. (1993), *vol.* 256, *pp.* 85–106

A critical-layer analysis of the resonant triad in boundary-layer transition: nonlinear interactions

By REDA R. MANKBADI[1], XUESONG WU[2] AND SANG SOO LEE[3]

[1] NASA Lewis Research Center, Cleveland, OH 44135, USA

[2] Department of Mathematics, Imperial College, 180 Queens Gate, London SW7 2BZ, UK

[3] Sverdrup Technology, Inc., Lewis Research Center Group, Cleveland, OH 44135, USA

(Received 17 May 1991 and in revised form 29 April 1993)

A systematic theory is developed to study the nonlinear spatial evolution of the resonant triad in Blasius boundary layers. This triad consists of a plane wave at the fundamental frequency and a pair of symmetrical, oblique waves at the subharmonic frequency. A low-frequency asymptotic scaling leads to a distinct critical layer wherein nonlinearity first becomes important, and the critical layer's nonlinear, viscous dynamics determine the development of the triad.

The plane wave initially causes double-exponential growth of the oblique waves. The plane wave, however, continues to follow the linear theory, even when the oblique waves' amplitude attains the same order of magnitude as that of the plane wave. However, when the amplitude of the oblique waves exceeds that of the plane wave by a certain level, a nonlinear stage comes into effect in which the self-interaction of the oblique waves becomes important. The self-interaction causes rapid growth of the phase of the oblique waves, which causes a change of the sign of the parametric-resonance term in the oblique-waves amplitude equation. Ultimately this effect causes the growth rate of the oblique waves to oscillate around their linear growth rate. Since the latter is usually small in the nonlinear regime, the net outcome is that the self-interaction of oblique waves causes the parametric resonance stage to be followed by an 'oscillatory' saturation stage.

1. Introduction

1.1. *Background*

Experiments on boundary-layer transition and accompanying instability-wave growth have identified several distinct flow-development regimes. The first regime begins with the onset of two-dimensional, Tollmien–Schlichting (TS) waves that at small amplitudes harmlessly grow and decay in accordance with the linear stability theory for a developing boundary layer. However, at larger amplitudes, a nonlinear, three-dimensional spanwise-periodic disturbance field appears. These three-dimensional disturbances grow at much higher rates than predicted by linear theory and ultimately lead to the transition to turbulence. For low-to-intermediate levels of two-dimensional disturbances, the nonlinear regime is characterized by the formation of a staggered, lambda-shaped structure indicating the appearance of a subharmonic of the input TS wave (Knapp & Roache 1968; Kachanov, Kozlov & Levchenko 1978; Kachanov & Levchenko 1984; Saric, Kozlov & Levchenko 1984; Corke & Mangano 1989). Since

this structure occurs at low-to-intermediate amplitudes of the TS wave, it is more likely to occur in natural transition than is the fundamental-type structure of Klebanoff, Tidstrom & Sargent (1962). The subject of the present work is, therefore, the subharmonic route to boundary-layer transition.

The observed three-dimensionality in boundary-layer transition has prompted several theoretical and numerical investigations. Raetz (1959) and Craik (1971) proposed the existence of a resonant triad consisting of a plane wave and a pair of symmetrical oblique waves. If the wavenumbers are such that the phase velocities are equal, then a strong interaction might occur, leading to a selective growth of a pair of oblique waves with a particular obliqueness angle. Craik's (1971) resonant triad thus established, in principle, the subharmonic route to boundary-layer transition. Smith & Stewart (1987) considered the resonant interactions in the high-frequency limit of the lower-branch scaling regime starting from the triple-deck equations where the critical layer is located in the viscous wall layer (lower deck). The linear secondary stability analysis of Herbert (1983, 1988) explained many features of the observed phenomena in the parametric-resonance stage of interaction. The parametric-resonance stage has also been studied by Mankbadi (1990) through analysing the critical-layer nonlinearity that results from the continual downstream growth of initially linear TS waves comprising a resonant triad. This analysis was inspired by an early version of Goldstein & Lee (1992), who first studied the nonlinear resonant-triad interaction in an adverse-pressure-gradient boundary layer by analysing the non-equilibrium critical layer. Their analysis revealed novel features that were not obtained before. The present analysis is along similar lines to that of Goldstein & Lee (1992) in that it includes the self-interaction of the oblique waves, which is proportional to the cubic amplitude of the oblique waves. Wu (1992) studied similar resonant-triad waves consisting of Rayleigh waves with $O(1)$ wavelength in an oscillatory Stokes layer. Further discussion of previous work on the subject is given in Craik (1985), Herbert (1988), and Kleiser & Zang (1991).

1.2. *Scope of present work*

In the present work a first-principles theory is developed for the study of a spatially evolving resonant triad in Blasius boundary-layer transition. The triad consists of a plane TS wave at the fundamental frequency ω and a pair of three-dimensional oblique waves at the subharmonic frequency $\frac{1}{2}\omega$. The oblique waves make equal and opposite angles $\pm\theta$ to the flow direction, and the oblique modes' common streamwise wavenumber is nearly one-half that of the plane wave. The growth rate of the triad's amplitudes is controlled by nonlinear interactions in the viscous critical layer and diffusion layer surrounding the transverse position where the wave's phase velocity equals the velocity of the mean flow.

Two stages of the nonlinear interaction can be identified in experimental observations on subharmonic-type transition: a parametric-resonance stage and a nonlinear stage. In the parametric-resonance (second-instability) stage, the subharmonic oblique waves experience a superexponential growth that is faster than the exponential growth predicted by the linear theory, but the fundamental plane wave follows the linear theory (Herbert 1988; Mankbadi 1990). This stage is followed by the nonlinear stage, wherein the subharmonic exceeds the fundamental and saturates. This latter stage has not yet been fully explored by direct numerical simulations owing to the resolution requirements that become prohibitive downstream. However, this stage is directly related to the final breakdown to turbulence, and exhibits several interesting features as have been observed in Corke & Mangano's (1989) experiment. The present study considers the nonlinear interaction of the waves, starting from the linear stage going

through the parametric-resonance and the nonlinear stages. Emphasis is on capturing the nonlinear stage, which is achieved by allowing the oblique waves to grow to amplitudes large enough to capture the self-interaction of the oblique waves. This stage has also been emphasized in Goldstein & Lee's (1992) analysis of a resonant triad of inviscid Rayleigh waves in an adverse-pressure-gradient boundary layer.

Subharmonic resonance has been observed experimentally to first occur near, and continue downstream of, the upper-branch neutral stability curve (see data of Kachanov & Levchenko 1984; Saric *et al.* 1984; Corke & Mangano 1989). The parametric resonance growth rate (that results from the fundamental–subharmonic interaction) is proportional to the plane wave's amplitude, which peaks at the upper branch. Furthermore, the present study reveals that the proportionality coefficient increases as the Reynolds number increases in the downstream direction. These two factors cause resonance to occur in vicinity and downstream of the upper branch, and the subharmonic maximum growth rate to occur downstream of the upper branch. It has been observed experimentally that if the upstream amplitude of the plane wave is forced to be large, the resonance location does not move upstream to the lower branch, and the Klebanoff-type of structure appears instead (Saric *et al.* 1984). Thus, the upper-branch scaling should be the appropriate one to adopt here for analysis of the subharmonic resonance phenomena. Upper-branch scaling leads to a multi-deck structure of the instability waves that is characterized by a distinct viscous/nonlinear critical layer separated from the viscous wall layer (Lin 1955; Bodonyi & Smith 1981), which cannot be captured by a triple-deck structure. Moreover, the upper-branch scaling is not restricted to the vicinity of the upper branch, but, as pointed out by Goldstein & Durbin (1986), at low dimensionless frequencies, covers most of the unstable Reynolds-number range, and breaks down only in an asymptotically small neighbourhood of the lower branch.

Experimental observations indicate that the subharmonic resonance phenomenon occurs at low dimensionless frequencies F. This is because at high frequencies the growth rates are small and the unstable domain is narrow; therefore, the plane wave cannot reach an amplitude large enough to trigger the resonance phenomenon (secondary instability). The phenomenon is thus important at low frequencies, and as such, it is appropriate to adopt here a low-frequency asymptotic scaling. The asymptotic solution is an expansion in terms of a small-frequency parameter $\sigma = (\omega\nu/U_\infty^2)^{\frac{1}{12}}$, the maximum of which at the highest frequency point in the neutral stability curve is about 0.5. Since the resonance phenomenon occurs at lower frequencies, it should be described accurately by such a low-frequency scaling.

The waves are taken to be initially describable by the spatial linear theory since observations on boundary-layer transitions reveal initially linear, harmonically time-dependent, spatially growing waves. The scaling and the linear solution are given in §2. The scaling leads to the multi-deck stability structure and brings into play the critical layer and distinguishes it from the viscous wall layer. Slowly varying amplitude functions are introduced in the linear solution and are ultimately determined by considering the nonlinear viscous flow in the critical layer. The linear solution in the different transverse zones of the boundary layer is obtained, and matching the solution in the different transverse zones leads to a linear relationship between the growth rate and the velocity jump across the critical layer.

The continued downstream growth of the instability waves results in nonlinearity, which first appears in the nearly common critical layer. The appearance of nonlinearity in the critical layer was first pointed out by Lin (1957) and Benney & Bergeron (1969) and is supported by experimental observations, such as those of Corke & Mangano

(1989), which show that the nonlinearity is concentrated in the critical layer. Maslowe (1986) is an excellent review of critical layers in shear flows.

Section 3 addresses the nonlinear, viscous critical-layer flow. If the scale of the oblique waves' amplitude was taken to be the same order of magnitude as or less than that of the plane wave, the plane wave continues to follow the linear theory because the quadratic backreaction on it does not appear in its amplitude equation. However, the presence of the plane wave causes a double-exponential growth for the oblique waves with the effect of the oblique waves' self-interaction absent (Mankbadi 1990). However, the scales are determined in §3 such that the self-interaction of the oblique waves is captured. This requires allowing the oblique waves to continue to grow in the linear and resonance stages up to the first order of magnitude at which their amplitude becomes large enough to produce self-interaction. It is shown in §3 that the interaction produces a jump across the critical layer that corresponds to linear growth and to a parametric resonance interaction.

The interaction of the oblique waves in the critical layer produces a spanwise-periodic mean flow that cannot be matched directly to the outer layer and needs a diffusion layer (buffer layer) that sandwiches the critical-layer. The solution for the diffusion-layer flow is given in §4. The dominant balance in the diffusion layer is between the slow growth and the viscous effects. This nonlinearly generated mean flow interacts with the lowest-order oblique waves to produce a self-interaction term. The amplitude equations are then obtained in §5 by equating the velocity jump obtained from the nonlinear, viscous flow to the one obtained from the linear, outer solution. This yields a direct, nonlinear relationship between the growth rates and the amplitudes.

Results are presented in §6 with the weak flow-divergence effects suppressed by freezing Reynolds number. This is asymptotically correct because of the high Reynolds number and the comparatively short streamwise distance wherein nonlinearity occurs. The two stages of the interaction are illustrated. In the first stage the plane wave continues to follow the linear theory but causes a double-exponential growth of the oblique waves. However, as the oblique waves continue to grow to the extent that their amplitude exceeds that of the plane wave by a certain level, the nonlinear stage comes into effect. The self-interaction of oblique waves becomes a significant mechanism which causes an explosive growth of the phase angle of the oblique waves indicating a rapid change of its streamwise wavenumber. This causes the parametric resonance term to change sign and ultimately leads to a net growth rate that is in effect an oscillation around the linear growth rate. If the local linear growth rate of the oblique waves is zero then the self-interaction mechanism leads to oscillatory saturation.

2. Scaling and linear solution

Details of the linear solution are given in Mankbadi (1990); we limit the results here to those relevant to the nonlinear solution. The base flow is an incompressible laminar boundary layer with Blasius mean velocity U_B, where

$$U_B = \lambda y - \frac{\lambda^2}{2.4!} y^4 + \ldots \quad \text{as } y \to 0, \tag{1}$$

and $\lambda = 0.332$ denotes the scaled Blasius skin friction. The unsteady flow starts out as a resonant triad of spatially growing instability waves: a two-dimensional mode of normalized frequency ω and wavenumber α, and a pair of subharmonic oblique waves of frequency $\frac{1}{2}\omega$, streamwise wavenumber nearly equal to $\frac{1}{2}\alpha$, and spanwise wavenumber

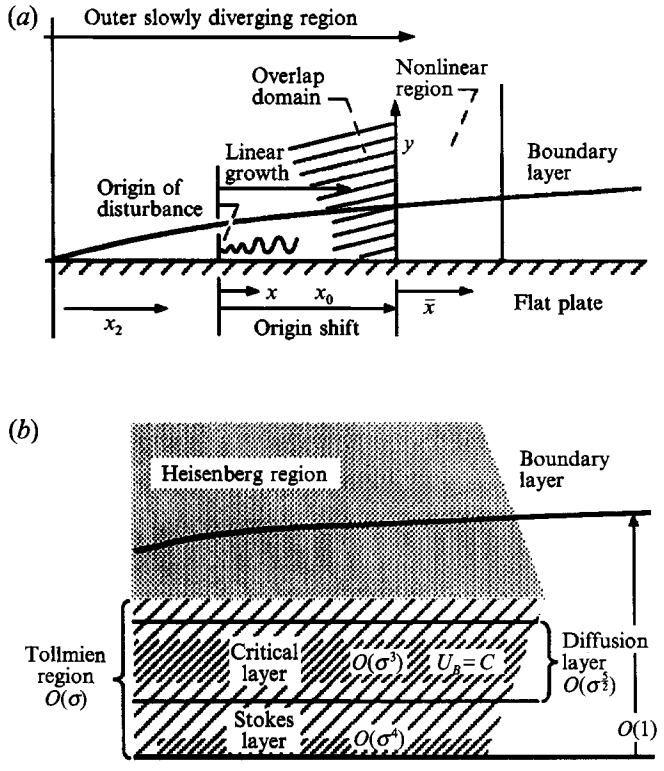

FIGURE 1. (*a*) Flow structure. (*b*) Stability wave structure.

$\pm\beta$. Upstream of the nonliner region (figure 1*a*) the waves evolve according to weakly non-parallel flow linear theory. All velocities are normalized by the free-stream velocity U_∞, lengths by δ_*, time by δ_*/U_∞, and pressure by ρU_∞^2, where ρ is the fluid density, $\delta_* = (\nu x/U_\infty)^{\frac{1}{2}}$ is the boundary-layer thickness, and ν is the kinematic viscosity.

The small-frequency parmeter σ is related to the normalized dimensionless frequency F by the relation (Goldstein & Durbin 1986)

$$F = \frac{\omega\nu}{U_\infty^2} \equiv \sigma^{12}, \tag{2}$$

and the Reynolds number scales as

$$\bar{R} = \sigma^{10} R, \tag{3}$$

where R is the Reynolds number based on the local thickness δ_* and the overbar denotes an order-one scaled quantity. The normalized, complex wavenumber α is small, and its imaginary part is even smaller than its real part. Consequently, each of the three waves has a well-defined critical layer at nearly the same transverse position, y_c, where the real part of their nearly common phase velocity, c, equals the streamwise velocity $U(y_c)$. In the upper-branch scaling $\alpha = \sigma\bar{\alpha} + \ldots$, $c = \sigma\bar{c} + \ldots$, where $\bar{\alpha}$ and $\bar{c}$ are order-one real constants. Outside the critical layer, the unsteady flow is governed by linear dynamics, and the velocity field is given by

$$u = U_B(y) + \mathrm{Re}\{\epsilon A_0(x_1)\,\Phi_{0,y}(y, x_1, \sigma)\,\mathrm{e}^{\mathrm{i}X} + \delta A(x_1)[U_+(y, x_1, \sigma)\,\mathrm{e}^{\mathrm{i}Z} + U_-(y, x_1, \sigma)\,\mathrm{e}^{-\mathrm{i}Z}]\,\mathrm{e}^{\frac{1}{2}\mathrm{i}X}\}, \tag{4}$$

$$v = -\mathrm{Re}\{\mathrm{i}[\epsilon\alpha A_0\,\Phi_0\,\mathrm{e}^{\mathrm{i}X} + 2\delta\gamma A\Phi\cos Z\,\mathrm{e}^{\frac{1}{2}\mathrm{i}X}]\}, \tag{5}$$

$$w = \mathrm{Re}\{\delta A(W_+ e^{iZ} + W_- e^{-iZ}) e^{\frac{1}{2}iX}\}, \tag{6}$$

where

$$X \equiv \sigma\bar{\alpha}(x - \sigma\bar{c}t), \quad Z \equiv \sigma\bar{\beta}z, \tag{7}$$

$$\bar{\gamma} \equiv [(\bar{\alpha}/2)^2 + \bar{\beta}^2]^{\frac{1}{2}}, \tag{8}$$

$$x_1 \equiv \sigma^4 x, \tag{9}$$

and Re denotes the real part. A multiple scale procedure is used and the slow scale x_1 is introduced. In the above equations the scaled amplitudes A_0 and A are for the two-dimensional and the oblique waves, respectively, and ϵ and δ are their corresponding order of magnitudes. The amplitudes will ultimately be determined from the nonlinear analysis in the critical layer. Because the initial development of the instability waves is linear, we can take $A(x_1)$ to be a real quantity initially, but we allow $A_0(x_1)$ to be complex to account for possible wavenumber detuning. Farther downstream the nonlinear effects cause both $A(x_1)$ and $A_0(x_1)$ to be complex. In (4) and (6), $U_\pm$ and $W_\pm$ satisfy the relations

$$[(\gamma^2 - \beta^2)^{\frac{1}{2}}/\gamma]\, U_\pm \pm (\beta/\gamma)\, W_\pm = \Phi_y, \tag{10}$$

$$(\beta/\gamma)\, U_\pm \mp [(\gamma^2 - \beta^2)^{\frac{1}{2}}/\gamma]\, W_\pm = [\beta/(\gamma^2 - \beta^2)^{\frac{1}{2}}]\, \Phi U_y/(U - c), \tag{11}$$

and $\Phi_0(\alpha, c_0, y)$ and $\Phi(\gamma, c, y)$ satisfy the corresponding Orr–Sommerfeld equations subject to the usual boundary conditions $\Phi = \Phi_y = \Phi_0 = \Phi_{0,y} = 0$ at $y = 0$. The wavenumbers and phase velocities scale to the required order of approximation as (see Goldstein, Durbin & Leib 1987)

$$\alpha = \sigma\bar{\alpha} + \sigma^4 \frac{A_0'}{iA_0}, \quad \gamma = \sigma\bar{\gamma} + \frac{\sigma^4}{2i}\frac{\bar{\alpha}}{\bar{\gamma}}\frac{A'}{A}, \quad \beta = \sigma\bar{\beta}, \tag{12}$$

$$c_0 = \frac{\sigma\bar{c}}{1 + \dfrac{\sigma^3}{i\bar{\alpha}}\dfrac{A_0'}{A_0}}, \quad c = \frac{\sigma\bar{c}}{1 + 2\dfrac{\sigma^3}{i\bar{\alpha}}\dfrac{A'}{A}}, \tag{13}$$

$$\bar{c} = \bar{R}/\bar{\alpha}. \tag{14}$$

Here, the prime denotes differentiation with respect to the slow variable x_1. The scaling (2), (3) and (14) are consistent with Reid's (1965) equation (3.128).

In the high-Reynolds-number limit, the unsteady flow solution exhibits a multi-zoned structure (figure 1*b*), in which the critical layer is distinct from the viscous wall layer (see Bodonyi & Smith 1981; Drazin & Reid 1981, p. 166; and references therein). Zone I closest to the wall (Stokes layer) is a viscous layer. Zone II (Tollmien region) is an inviscid, rotational layer of adjustment, within which the viscous critical layer zone III is induced. Zone IV is above zone II and is an inviscid rotational region comprising most of the boundary layer. Above zone IV is the quasi-steady zone V, in which the flow properties are inviscid and irrotational ($U = 1, V = 0$). Zones IV and V can be combined into one zone (Heisenberg region). As will be seen in §4 a diffusion layer that sandwiches the critical layer is needed to match the mean flow generated in the critical layer to the outer flow. Matching the linear solutions in zones II and IV produces the relations

$$\left(\cos\theta + \frac{1}{\cos\theta}\right)\frac{A'}{A} = \frac{(\bar{\gamma}\bar{c})^2}{4\lambda^3}(\Delta\phi) + \frac{\bar{\gamma}^2}{\bar{c}^2(\bar{c}\bar{R}\bar{\alpha})^{\frac{1}{2}}}, \tag{15}$$

$$\frac{A_0'}{A_0} = \frac{(\bar{\alpha}\bar{c})^2}{8\lambda^3}(\Delta\phi_0) + \frac{\bar{\alpha}^2}{2\bar{c}^2(2\bar{c}\,\bar{R}\alpha)^{\frac{1}{2}}}, \tag{16}$$

$$\bar{\gamma} = \bar{\alpha} + O(\sigma^3), \tag{17}$$

$$\lambda\bar{c} = \bar{\alpha} + O(\sigma). \tag{18}$$

Here $\Delta\phi$ and $\Delta\phi_0$ are the velocity jumps across the critical layer (and diffusion layer) for the oblique and plane waves, respectively, and y_c is the location of the critical layer, which scales as

$$y_c = \sigma Y_c. \tag{19}$$

In the Tollmien region, the scaled transverse coordinate $y = \sigma Y$, Y is $O(1)$, is introduced directly into the Orr–Sommerfeld equation before attempting to obtain the solution in this region. The obliqueness angle θ is defined as

$$\theta \equiv \sin^{-1}(\bar{\beta}/\bar{\gamma}). \tag{20}$$

Upon substituting (8) and (17) into (20), we obtain

$$\theta = 60° \tag{21}$$

for the perfect tuning case.

The velocity field in zone II, which contains the critical layer, is given according to the linear solution as

$$u = \sigma\lambda Y - \sigma^4 \frac{\lambda^2}{2.4!} Y^4 + \mathrm{Re}\{[\lambda + \sigma a_0 + \sigma^3(f + \mathrm{i}\mu Y_c \phi_0^{\pm})]\,\epsilon A_0 \mathrm{e}^{\mathrm{i}X} + 2\delta A g(\cos Z)\,\mathrm{e}^{\frac{1}{2}\mathrm{i}X}\} + \ldots, \tag{22}$$

$$v = -\mathrm{Re}\,\sigma^2\lambda Y[\mathrm{i}\bar{\alpha}\epsilon A_0 \mathrm{e}^{\mathrm{i}X} + 2\mathrm{i}\bar{\gamma}\delta A(\cos Z)\,\mathrm{e}^{\frac{1}{2}\mathrm{i}X}] + \ldots, \tag{23}$$

$$w = -\mathrm{Re}\,2\mathrm{i}\delta\bar{c}\lambda\Upsilon A(\sin\theta\sin Z)\,\mathrm{e}^{\frac{1}{2}\mathrm{i}X} + \ldots, \tag{24}$$

$$p = \mathrm{Re}\,\sigma\bar{c}\lambda[\epsilon A_0 \mathrm{e}^{\mathrm{i}X} + 2\delta A(\cos\theta\cos Z)\,\mathrm{e}^{\frac{1}{2}\mathrm{i}X}] + \ldots, \tag{25}$$

where

$$\begin{aligned} g = {} & \frac{\lambda + \sigma a}{\cos\theta} + \bar{c}(\lambda + \sigma a)\,\Upsilon(\sin\theta\tan\theta) + \sigma^3\left(f\cos\theta + \sin\theta\tan\theta\Upsilon\left\{\lambda F(0)\right.\right. \\ & + \mu\lambda Y_c[(Y - Y_c)\ln|Y - Y_c| + Y_c \ln Y_c \\ & \left.\left. + \lambda Y^2\left[\frac{\mu}{2} - \frac{\lambda^2 Y}{4!}(Y_c + 2Y - \bar{c}Y\tfrac{1}{2}Y)\right]\right\} \\ & + \frac{\lambda A'}{\bar{\gamma}\mathrm{i}A}\sin^2\theta\left[1 - \lambda Y\Upsilon\left(1 + \frac{\lambda Y\Upsilon}{\cos^2\theta}\right)\right] + \frac{\mathrm{i}\mu Y_c}{\cos\theta}(\phi^{\pm} + \bar{c}\Upsilon\phi^{-}\sin^2\theta)\right), \end{aligned} \tag{26}$$

$$f = \mu(Y + Y_c + Y_c \ln|Y - Y_c|) - \tfrac{1}{2}\lambda^2 Y^2\left(\frac{Y_c}{4} + \frac{Y}{3!}\right), \tag{27}$$

$$\Upsilon = 1/(\lambda Y - \bar{c}), \quad \mu = -\lambda^2 Y_c^2/4. \tag{28}$$

3. Nonlinear, viscous flow in critical layer

The previous linear solution (22)–(25), becomes singular at the critical point. The appropriate transverse scaled coordinate in this region (Lin 1955) is given by

$$\bar{\eta} = (Y - Y_c)/\sigma^2. \tag{29}$$

On substituting (29) into (22)–(25), we find that the critical-layer solution expands as

$$\begin{aligned} u - \sigma\bar{c} = {} & \sigma^3\lambda\bar{\eta} + \tfrac{1}{3}\sigma^6\mu Y_c\bar{\eta} + \tfrac{1}{2}\sigma^8\mu\bar{\eta}^2 + \delta(\sigma^{-2}u_{-2} + \sigma^{-1}u_{-1} + u_0 + \sigma u_1 + \sigma^2 u_2 + \ldots) \\ & + \epsilon(u_{0,0} + \sigma u_{0,1} + \sigma^2 u_{0,2} + \sigma^3 u_{0,3} + \ldots) + \ldots, \end{aligned} \tag{30}$$

$$\bar{v} = -\mathrm{Re}[\epsilon\sigma^{-2}\bar{\alpha}\lambda Y_c \mathrm{i}A_0 \mathrm{e}^{\mathrm{i}X} + 2\delta\sigma^{-2}\bar{\gamma}\lambda Y_c(\cos Z)\mathrm{i}A\,\mathrm{e}^{\frac{1}{2}\mathrm{i}X}] + \ldots, \tag{31}$$

$$w = \delta(\sigma^{-2}w_{-2} + \sigma^{-1}w_{-1} + w_0 + \sigma w_1 + \sigma^2 w_2 + \sigma^3 w_3 + \ldots), \tag{32}$$

$$p = \mathrm{Re}[\epsilon\sigma\lambda\bar{c}A_0 \mathrm{e}^{\mathrm{i}X} + 2\delta\sigma\lambda\bar{c}\cos\theta\cos Z A\,\mathrm{e}^{\frac{1}{2}\mathrm{i}X}] + \ldots, \tag{33}$$

where u and u_0 denote the oblique and plane waves respectively, and

$$v \equiv \sigma^4 \bar{v}, \quad \bar{c} = \lambda Y_c + O(\sigma^3). \tag{34}$$

The momentum equations can be expressed in terms of the scaled variables x_1, X, Z, and $\bar{\eta}$ as (Mankbadi 1990)

$$\left\{\bar{\alpha}(u-\sigma\bar{c})\frac{\partial}{\partial X}+\bar{v}\frac{\partial}{\partial\bar{\eta}}+\bar{\beta}w\frac{\partial}{\partial Z}+\sigma^3 u\frac{\partial}{\partial x_1}-\frac{\sigma^3}{\bar{R}}\frac{\partial^2}{\partial\bar{\eta}^2}\right\}(u,\bar{v},w) = -(\bar{\alpha}p_X+\sigma^3 p_{x_1}, \sigma^{-8}P_{\bar{\eta}}, \bar{\beta}p_Z), \tag{35}$$

and the continuity equation as

$$\bar{\alpha}u_X+\bar{v}_{\bar{\eta}}+\bar{\beta}w_Z+\sigma^3 u_{x_1} = 0. \tag{36}$$

The scale of the plane wave amplitude that produces a parametric resonance term in the oblique-wave equation is given by

$$\epsilon = \sigma^{10}. \tag{37}$$

As for the oblique waves, taking $\delta \leqslant \epsilon$, as was done in Mankbadi (1990), captures the parametric resonance stage, but not the subsequent stage where the self-interaction of oblique waves becomes important. To capture the latter stage, a larger scaling of the oblique waves amplitude is needed, namely

$$\delta = \epsilon/\sigma^2 = \sigma^8. \tag{38}$$

As outlined below, the above scaling arises from considering the interaction of the oblique waves in the critical layer and the diffusion layer. The nonlinear interaction in the critical layer produces a spanwise-periodic mean flow (02) that cannot be matched directly to the outer layer. Therefore, we introduce a diffusion layer (buffer layer) that sandwiches the critical-layer. The dominant balance in the diffusion layer is between the slow growth and the viscous effects. This nonlinearly generated mean flow, which is unbounded in the critical layer, interacts with the lowest-order oblique waves in the diffusion layer to produce a self-interaction term. The requirement that this term be of the same order as the linear and parametric resonance terms determines the scaling of the oblique waves amplitude.

Substituting (37) and (38) into (30)–(33) allows one to rewrite the expansions in the general form

$$\begin{aligned} u-\sigma\bar{c} &= \sigma^3\lambda\bar{\eta}+\sigma^6 U_6+\sigma^7 U_7+\sigma^8 U_8+\sigma^9 U_9\ldots, \\ \bar{v} &= \sigma^6 V_6+\sigma^7 V_7+\sigma^8 V_8+\sigma^9 V_9+\ldots, \\ w &= \sigma^6 W_6+\sigma^7 W_7+\sigma^8 W_8+\sigma^9 W_9+\ldots, \\ p &= \sigma^9 P_9+\sigma^{10}P_{10}+\sigma^{11}P_{11}+\sigma^{12}P_{12}+\ldots. \end{aligned} \tag{39}$$

The Blasius mean flow components at the order σ^6 and σ^8 are given by

$$\bar{U}_6 = \tfrac{1}{3}\mu Y_c\bar{\eta}, \quad \bar{U}_8 = \tfrac{1}{2}\mu\bar{\eta}^2, \tag{40}$$

and the outer linear solution gives for the oblique and plane wave components, respectively,

$$(V_6, P_9)_{3D} = \mathrm{Re}\,\lambda(-\mathrm{i}\bar{\gamma}Y_c, \bar{c}\cos\theta)\,2(\cos Z)A\,\mathrm{e}^{\frac{1}{2}\mathrm{i}X}, \tag{41}$$

$$(V_8, P_{11})_{2D} = \mathrm{Re}\,\lambda(-\mathrm{i}\bar{\alpha}Y_c, \bar{c})\,A_0\,\mathrm{e}^{\mathrm{i}X}. \tag{42}$$

Substituting (39) into (35) and (36), we obtain the following equations for each term

in the expansion (39) that describe the nonlinear viscous flow in the critical layer, for $L = 6, 7, 8, \ldots$

$$\mathscr{L}_3 U_L = -\lambda V_L - \sum_{K=4}^{L} \mathscr{L}_K U_{(3+L-K)} - \bar{\alpha} P_{(3+L),X} - P_{L,x_1},$$

$$\mathscr{L}_3 W_L = -\sum_{K=4}^{L} \mathscr{L}_K W_{(3+L-K)} - \bar{\beta} P_{(3+L),Z}, \tag{43}$$

$$V_{L,\bar{\eta}} = -[\bar{\alpha} U_{L,X} + \bar{\beta} W_{L,Z} + U_{(L-3),x_1}],$$

where

$$\mathscr{L}_3 = \bar{\alpha}\lambda\bar{\eta}\frac{\partial}{\partial X} - \frac{1}{\bar{R}}\frac{\partial^2}{\partial\bar{\eta}^2}, \quad \mathscr{L}_4 = \bar{c}\frac{\partial}{\partial x_1}, \quad \mathscr{L}_5 = 0,$$

$$\mathscr{L}_6 = \bar{\alpha} U_6 \frac{\partial}{\partial X} + V_6 \frac{\partial}{\partial\bar{\eta}} + \bar{\beta} W_6 \frac{\partial}{\partial Z} + \lambda\bar{\eta}\frac{\partial}{\partial x_1},$$

$$\mathscr{L}_K = \bar{\alpha} U_K \frac{\partial}{\partial X} + V_K \frac{\partial}{\partial\bar{\eta}} + \bar{\beta} W_K \frac{\partial}{\partial Z} + U_{K-3}\frac{\partial}{\partial x_1}, \quad K = 7, 8, \ldots, \tag{44}$$

$$U_K = V_K = W_K = P_{K+3} = 0 \quad \text{for } K = 3, 4, 5.$$

3.1. *Jump across the critical-layer*

The amplitude equations are derived by equating the velocity jump across the critical layer and diffusion layer to that obtained from the outer linear solution (Mankbadi 1990).

3.1.1. *Oblique waves*

The amplitude equation is obtained by equating the velocity jump from the nonlinear solution (39) with that from the outer linear solution (22)–(25). For the oblique waves this jump occurs at the U_{11} level. The equation for $U^+_{11,\bar{\eta}}$, obtained from (43), is

$$\mathscr{L}_3 U^+_{11,\bar{\eta}} = \lambda D^+ W_{11} - (\lambda\bar{\eta} U^+_8 + \bar{c} U^+_{10})_{\bar{\eta}x_1} + \lambda(\cos\theta) U_{8,x_1} - \sum_{K=6}^{8} \bar{\alpha} U_{14-K} U^+_{K,X} + \bar{\beta} W_{14-K} U^+_{K,Z} + V_{14-K} U^+_{K,\bar{\eta}})_{\bar{\eta}}, \tag{45}$$

where

$$U^+_K = U_K \cos\theta + W_K \sin\theta, \tag{46}$$

and

$$D^+ = \cos\theta\bar{\beta}\frac{\partial}{\partial Z} - \sin\theta\bar{\alpha}\frac{\partial}{\partial X}. \tag{47}$$

The solution for $U^+_{11,\bar{\eta}}$ can be written in the general form

$$U^+_{11,\bar{\eta}} = \mathrm{Re}\sum_{n,m} Q^{(nm)}_{11}(\bar{\eta}, x_1)\, e^{i(\frac{1}{2}nX + mZ)}. \tag{48}$$

Since the velocity jump from the outer solution to be matched is composed only of oblique waves of the form $\sim \exp(\frac{1}{2}iX \pm iZ)$, only the solution of $U^+_{11,\eta}$ corresponding to $n = 1$ and $m = 1$ is needed.

The lowest-order solution for the oblique waves at the 6-level can be written as

$$(U_6, W_6)_{3D} = 2\,\mathrm{Re}(i\tan\theta\cos Z, \sin Z)\, Q(\bar{\eta}, x_1)\, e^{\frac{1}{2}iX}, \tag{49}$$

where Q satisfies

$$\left(\tfrac{1}{2}i\bar{\alpha}\lambda\bar{\eta} - \frac{1}{\bar{R}}\frac{\partial^2}{\partial\bar{\eta}^2}\right) Q = \bar{\gamma}\lambda\bar{c}A\sin\theta\cos\theta. \tag{50}$$

Using Fourier transform in $\bar{\eta}$, we obtain

$$Q = A(\bar{x})\sin\theta \int_{-\infty}^{0} \exp(\mathrm{i}K\eta + \tfrac{1}{3}hK^3)\,\mathrm{d}K, \tag{51}$$

where $$\eta = \bar{\eta}/\bar{c}, \quad h = 2/(\bar{\alpha}\lambda\bar{c}^3\bar{R}), \quad \bar{x} = x_1 - x_0, \tag{52}$$

and x_0 is the origin of the nonlinear region. Substituting the lower-order solution into (45) we obtain $Q_{11}^{(11)}$ and its Fourier transform $\hat{Q}_{11}^{(11)}(K)$. The velocity jump for the three-dimensional wave, is given by

$$J_{3D} = \int_{-\infty}^{\infty} Q_{11}^{(11)}\,\mathrm{d}\bar{\eta} = \hat{Q}_{11}^{(11)}(K=0), \tag{53}$$

which yields

$$J_{3D} = -\bar{c}\left(\frac{\mathrm{i}\pi\bar{R}}{4\lambda^2}A + \frac{3\pi\bar{R}^2}{4}A_0 A^*\right). \tag{54}$$

3.1.2. *The two-dimensional wave*

Comparing the expansion (39) with the linear solution (22)–(25) indicates that the velocity jump for the two-dimensional wave occurs at the level of U_{13}. The equation for U_{13} is obtained from (43) as

$$\mathscr{L}_3 U_{13\bar{\eta}}^{+} = \lambda D^{+} W_{13} - (\lambda\bar{\eta}U_{10}^{+} + \bar{c}\,U_{12}^{+})\bar{\eta}x_1 - (U_6\,U_{7,x_1}^{+} + U_7\,U_{6,x_1}^{+})_{\bar{\eta}}$$
$$+ \lambda(\cos\theta)U_{10,x_1} - \sum_{K=6}^{10}(\bar{\alpha}U_{16-K}\,U_{K,X}^{+} + \bar{\beta}W_{16-K}\,U_{K,Z}^{+} + V_{16-K}\,U_{K,\bar{Z}}^{+})_{\bar{\eta}}. \tag{55}$$

The general solution for (55) is in the form

$$U_{13,\bar{\eta}}^{+} = \mathrm{Re}\sum_{n,m} Q_{13}^{(nm)}(\bar{\eta}, x_1)\exp[\mathrm{i}(\tfrac{1}{2}nX + mZ)]. \tag{56}$$

We need to obtain $Q_{13}^{(20)}$ in order to match the critical layer jump to the outer one. The procedure is similar to that outlined in §3.1.1. The jump for the two-dimensional wave, J_{2D}, is obtained as

$$J_{2D} = \int_{-\infty}^{\infty} Q_{13}^{(20)}\,\mathrm{d}\bar{\eta} = -\frac{\mathrm{i}\pi}{8}\frac{\bar{c}\bar{R}}{\lambda^2}A_0. \tag{57}$$

An A^2 term appears on the right-hand side of equation (55) but it was found not to produce a jump across the critical layer, as was first shown in Goldstein & Lee (1992).

3.2. *Mean flow generated in the critical layer*

The interaction of the oblique waves ($\delta = \sigma^8$) in the critical layer generates two-dimensional mean flow of the form (00) and spanwise-periodic mean flow of the form (02). However, the (02) flow component becomes unbounded outside the critical layer. A diffusion layer (buffer layer) is required for its matching to the outer flow. In fact, this is a characteristic of an equilibrium critical layer of three-dimensional modes, as noted by Brown, Brown & Smith (1993), and Wu, Lee & Cowley (1993). We consider herein the generated (02) flow component which is required to determine the diffusion-layer solution. The generated (02) flow is governed by

$$-\frac{1}{\bar{R}}\frac{\partial^2}{\partial\bar{\eta}^2}W_9^{(02)} = \mathrm{i}2\bar{\beta}QQ^* - \tfrac{1}{2}\lambda Y_c\bar{\gamma}(A^*Q_{\bar{\eta}} - AQ_{\bar{\eta}}^*), \tag{58}$$

$$V_{9,\bar{\eta}}^{(02)} = -2\mathrm{i}\bar{\beta}W_9^{(02)}, \tag{59}$$

$$-\frac{1}{\bar{R}}\frac{\partial^2}{\partial\bar{\eta}^2}U_9^{(02)} = -\lambda V_9^{(02)} + \frac{\lambda Y_c\bar{\gamma}\bar{\beta}}{\bar{\alpha}}(A^*Q_{\bar{\eta}} + AQ_{\bar{\eta}}^*), \tag{60}$$

where we have put $(U_9, V_9, W_9) = \mathrm{Re}(U_9^{(02)}, V_9^{(02)}, W_9^{(02)})\,\mathrm{e}^{2\mathrm{i}Z} + \ldots$. As $\bar{\eta}$ goes to $\pm\infty$, we can show that

$$Q \to -\mathrm{i}\frac{\bar{c}}{\bar{\eta}} A \sin\theta, \tag{61}$$

$$W_9^{(02)} \to |A|^2(C_1 \ln|\bar{\eta}| \pm C\bar{\eta} + C_2), \tag{62}$$

$$U_9^{(02)} \to -2\mathrm{i}\bar{\beta}\lambda\bar{R}|A|^2[\pm C(\bar{\eta}^4/4!) + C_1(\bar{\eta}^3/3!)\ln|\bar{\eta}| + \ldots], \tag{63}$$

where C_1 is given by

$$C_1 = -\mathrm{i}\bar{c}^2\overline{\gamma R}\sin\theta\cos 2\theta, \tag{64}$$

and the coefficient C is obtained by integrating equation (58) as follows:

$$2|A|^2 C = \frac{\partial W_9^{(02)}}{\partial\bar{\eta}}\bigg|_{-\infty}^{\infty} = -4\pi\mathrm{i}\bar{\beta}\bar{c}|A|^2\bar{R}\sin^2\theta\int_{-\infty}^{0}\exp(\tfrac{2}{3}hK^3)\,\mathrm{d}K \tag{65}$$

which gives

$$C = -2\mathrm{i}\frac{\pi}{6^{\frac{2}{3}}}\Gamma(\tfrac{1}{3})\,\bar{c}\bar{\beta}\bar{R}^2\sin^2\theta. \tag{66}$$

Because these flow components become unbounded as $\bar{\eta}\to\pm\infty$, a diffusion layer is required to match them to the Tollmien region.

4. Diffusion-layer flow

The dominant balance in the diffusion layer is between the slow growth and the viscous effects, which determines the diffusion-layer scale as

$$\bar{\bar{\eta}} = (y - y_c)/\sigma^{\frac{5}{2}}. \tag{67}$$

The momentum and continuity equations for the diffusion-layer flow become, respectively,

$$\left\{\bar{\alpha}(U-\sigma\bar{c})\frac{\partial}{\partial X} + \bar{\bar{V}}\frac{\partial}{\partial\bar{\bar{\eta}}} + \bar{\beta}W\frac{\partial}{\partial Z} + \sigma^3 U\frac{\partial}{\partial x_1} - \frac{\sigma^4}{\bar{R}}\frac{\partial^2}{\partial\bar{\bar{\eta}}^2}\right\}(U, \bar{\bar{V}}, W) =$$

$$-(\bar{\alpha}P_X + \sigma^3 P_{x_1}, \sigma^{-7}P_{\bar{\bar{\eta}}}, \bar{\beta}P_Z), \tag{68}$$

$$\bar{\alpha}\frac{\partial U}{\partial X} + \frac{\partial\bar{\bar{V}}}{\partial\bar{\bar{\eta}}} + \bar{\beta}\frac{\partial W}{\partial Z} + \sigma^3\frac{\partial U}{\partial x_1} = 0, \tag{69}$$

where we have put

$$V \equiv \sigma^{\frac{7}{2}}\bar{\bar{V}}. \tag{70}$$

The expansion in the diffusion layer can be written as

$$\begin{aligned} U &= \sigma\bar{c} + \sigma^{2.5}\lambda\bar{\bar{\eta}} - \sigma^{5.5}\lambda^2 Y_c^3\bar{\bar{\eta}}/(2.3!) + \sigma^{6.5}U_{6.5} + \sigma^7 U_7 + \sigma^{7.5}U_{7.5} + \ldots, \\ \bar{\bar{V}} &= \sigma^{6.5}V_{6.5} + \sigma^7 V_7 + \sigma^{7.5}V_{7.5} + \ldots, \\ W &= \sigma^{6.5}W_{6.5} + \sigma^7 W_7 + \sigma^{7.5}W_{7.5} + \ldots. \end{aligned} \tag{71}$$

Equation (68) can now be written in the form:

$$\left.\begin{aligned} \lambda\bar{\alpha}\bar{\bar{\eta}}\,U_{6.5,X} + \lambda V_{6.5} &= -\bar{\alpha}P_{9,X}, \\ \lambda\bar{\alpha}\bar{\bar{\eta}}\,W_{6.5,X} &= -\bar{\beta}P_{9,Z}, \end{aligned}\right\} \tag{72}$$

and

$$\bar{\alpha}U_{6.5,X} + V_{6.5,\bar{\bar{\eta}}} + \bar{\beta}W_{6.5,Z} = 0. \tag{73}$$

The solution at the lowest order is given by

$$\left.\begin{aligned} U_{6.5} &= 2\sin\theta\tan\theta\cos Z(\bar{c}/\bar{\eta})\,\mathrm{Re}\,A\,\mathrm{e}^{\frac{1}{2}\mathrm{i}X},\\ V_{6.5} &= -2\bar{\gamma}\bar{c}\cos Z\,\mathrm{Re}\,\mathrm{i}A\,\mathrm{e}^{\frac{1}{2}\mathrm{i}X},\\ W_{6.5} &= -2\sin\theta\sin Z(\bar{c}/\bar{\eta})\,\mathrm{Re}\,\mathrm{i}A\,\mathrm{e}^{\frac{1}{2}\mathrm{i}X}. \end{aligned}\right\} \tag{74}$$

4.1. *The mean flow $U^{(02)}$ in the diffusion layer*

The first term of $U_9^{(02)}$ in (63) that is generated at order σ^9 within the critical layer (equation (63)) induces a term of order σ^7 in the diffusion layer because it is proportional to $\bar{\eta}^4$, and the next term in (63) induces a term of order $\sigma^{7.5}\ln\sigma$ in the diffusion layer because it is proportional to $\bar{\eta}^3\ln\bar{\eta}$ as $\bar{\eta}\to\infty$. To calculate the flow in this region we first let

$$(U_L, V_L, W_L) = \mathrm{Re}\,(\bar{U}_L^{(02)}, \bar{V}_L^{(02)}, \bar{W}_L^{(02)})\,\mathrm{e}^{2\mathrm{i}Z} + \ldots. \tag{75}$$

The equation for $\bar{U}_L^{(02)}$ becomes

$$\left(\bar{c}\frac{\partial}{\partial x_1} - \frac{1}{\bar{R}}\frac{\partial^2}{\partial\bar{\eta}^2}\right)\bar{U}_L^{(02)} + \lambda\bar{V}_{L+\frac{1}{2}}^{(02)} = 0 \quad (L = 7, 7.5), \tag{76}$$

and the continuity equation becomes

$$\frac{\partial\bar{V}_{L+\frac{1}{2}}^{(02)}}{\partial\bar{\eta}} + 2\mathrm{i}\bar{\beta}\,\bar{W}_{L+\frac{1}{2}}^{(02)} = 0 \quad (L = 7, 7.5). \tag{77}$$

Combining (75) and (76) gives

$$\left(\bar{c}\frac{\partial}{\partial x_1} - \frac{1}{\bar{R}}\frac{\partial^2}{\partial\bar{\eta}^2}\right)\frac{\partial\bar{U}_L^{(02)}}{\partial\bar{\eta}} = 2\mathrm{i}\bar{\beta}\lambda\,\bar{W}_{L+\frac{1}{2}}^{(02)}, \tag{78}$$

and for $\bar{W}^{(02)}$ we obtain

$$\left(\bar{c}\frac{\partial}{\partial x_1} - \frac{1}{\bar{R}}\frac{\partial^2}{\partial\bar{\eta}^2}\right)\bar{W}_{L+\frac{1}{2}}^{(02)} = S_{w,\,L+\frac{1}{2}} \quad (L = 7, 7.5). \tag{79}$$

where

$$S_{w,\,8.5} = 0, \quad S_{w,\,9} = C_1\frac{|A|^2}{\bar{\eta}^2}. \tag{80}$$

The solution for $\bar{W}_{8.5}^{(02)}$ must satisfy the condition

$$\bar{W}_{8.5,\,\bar{\eta}}^{(02)} \to \pm C|A|^2 \quad \text{as } \bar{\eta}\to\pm 0, \tag{81}$$

and is given by

$$\bar{W}_{8.5,\,\bar{\eta}}^{(02)} = \frac{(\bar{R}\bar{c})^{\frac{1}{2}}}{2\pi^{\frac{1}{2}}}C\bar{\eta}\int_0^\infty \exp\left(-\frac{\bar{R}\bar{c}}{4x_2}\bar{\eta}^2\right)x_2^{-\frac{3}{2}}|A(x_1 - x_2)|^2\,\mathrm{d}x_2. \tag{82}$$

The solution for $U^{(02)}$ is then obtained in the form

$$\bar{U}_{7,\,\bar{\eta}\bar{\eta}}^{(02)} = \mathrm{i}\lambda\bar{\beta}C\left(\frac{\bar{R}}{\pi\bar{c}}\right)^{\frac{1}{2}}\bar{\eta}\int_0^\infty \frac{1}{x_2^{\frac{1}{2}}}|A(x_1 - x_2)|^2\exp\left(-\frac{\bar{R}\bar{c}}{4x_2}\bar{\eta}^2\right)\mathrm{d}x_2, \tag{83}$$

$$\bar{U}_7^{(02)} = \pm\left(\tfrac{1}{36}\right)^{\frac{1}{3}}\Gamma\left(\tfrac{1}{3}\right)\sin^2\theta\frac{4\pi\lambda\bar{\beta}^2\bar{R}}{\bar{c}}\int_0^\infty |A(x_1 - x_2)|^2 x_2\left\{\frac{2}{\pi^{\frac{1}{2}}}\int_{\frac{1}{2}(\bar{R}\bar{c})^{\frac{1}{2}}x_2^{-\frac{1}{2}}}^\infty \mathrm{e}^{-t^2}\,\mathrm{d}t - 1\right\}\mathrm{d}x_2. \tag{84}$$

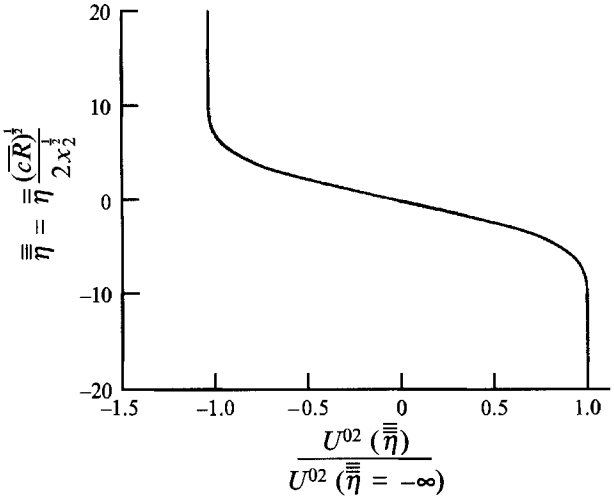

FIGURE 2. The mean flow (02) generated by the interaction of the oblique waves.

The normalized mean flow given by (84) is shown in figure 2, which indicates that it reaches a constant value outside the diffusion layer.

4.2. *Jump across the diffusion layer*

The streamwise component of the mean flow generated at order σ^7 interacts with the oblique wave at the leading order $\sigma^{6.5}$ to produce a jump across the diffusion layer at $O(\sigma^{11})$. The governing equation at this order is obtained from (72) as

$$\bar{\alpha}\lambda\bar{\bar{\eta}}\frac{\partial U_{11}^{+}}{\partial X} = -\bar{\alpha}U_7\frac{\partial U_{6.5}^{+}}{\partial X} - \bar{\beta}W_{6.5}\frac{\partial U_7}{\partial Z}\cos\theta - V_{6.5}\frac{\partial U_7}{\partial\bar{\bar{\eta}}}\cos\theta - \lambda V_{11}\cos\theta + \ldots, \tag{85}$$

where U_K^{+} is defined in (46). If we let

$$U_{11}^{+} = \mathrm{Re}\, U_{11}^{+(11)}(\bar{\eta}, x_1)\exp(\tfrac{1}{2}\mathrm{i}X + \mathrm{i}Z) + \ldots, \tag{86}$$

then the (11) component becomes

$$\bar{\bar{\eta}}U_{11,\bar{\bar{\eta}}}^{+(11)} = \frac{A\bar{c}}{2\lambda}\frac{\partial}{\partial\bar{\bar{\eta}}}\left(\frac{\partial\bar{U}_7^{(02)}}{\partial\bar{\bar{\eta}}} - 4\sin^2\theta\frac{\bar{U}_7^{(02)}}{\bar{\bar{\eta}}}\right) + \ldots. \tag{87}$$

The jump J across the diffusion layer can then be obtained from

$$J = \int_{-\infty}^{\infty} U_{11,\bar{\bar{\eta}}}^{+(11)}\,\mathrm{d}\bar{\bar{\eta}}. \tag{88}$$

Upon substituting (87) into (88) we obtain

$$J = A\frac{\bar{c}}{2\lambda}\cos 2\theta\int_{-\infty}^{\infty}\bar{U}_{7,\bar{\bar{\eta}}\bar{\bar{\eta}}}^{(02)}\frac{\mathrm{d}\bar{\bar{\eta}}}{\bar{\bar{\eta}}}. \tag{89}$$

Substituting (83) into (89) shows that the jump is given by

$$J = \mathrm{i}\bar{\beta}C\cos 2\theta A(x_1)\int_0^{\infty}|A(x_1 - x_2)|^2\,\mathrm{d}x_2. \tag{90}$$

Substituting for C from (66), we obtain

$$J = \frac{2\pi}{6^{\frac{2}{3}}}\Gamma(\tfrac{1}{3})(\cos 2\theta \sin^2\theta)\,\bar{c}\bar{\beta}^2\bar{R}^2 A(x_1)\int_0^\infty |A(x_1-x_2)|^2\,\mathrm{d}x_2, \tag{91}$$

where

$$\Gamma(\tfrac{1}{3}) = 2.6789 \tag{92}$$

denotes the Gamma function. Substituting

$$\bar{\beta} = \tfrac{1}{2}\bar{\alpha}\tan\theta, \quad \bar{\alpha} = (\lambda\bar{R})^{\frac{1}{2}}, \quad \bar{c} = (\bar{R}/\lambda)^{\frac{1}{2}}, \tag{93}$$

in (91) gives

$$J = \frac{\pi}{2.6^{\frac{2}{3}}\lambda^{\frac{1}{2}}}\Gamma(\tfrac{1}{3})\,\bar{\alpha}^2\sin^2\theta\cos 2\theta\tan^2\theta\bar{R}^{\frac{5}{2}}A(x_1)\int_0^\infty |A(x_1-x_2)|^2\,\mathrm{d}x_2. \tag{94}$$

The diffusion-layer dynamics are probably generic for three-dimensional disturbances. Similar analysis will be adopted in Wu (1993), wherein unequal amplitudes for the oblique-waves pair will be studied along with the structure of the mean-flow distortion. Results for the interaction of a plane wave with two pairs of oblique waves with frequencies detuned from the fundamental-subharmonic relation was given in Mankbadi (1991*a*, 1993).

5. The amplitude equations

The amplitude equations are obtained by equating the jump obtained from the linear solution to that obtained from the critical and diffusion layers. Rewriting (15) in the form

$$\frac{5}{2}\frac{\mathrm{d}A}{\mathrm{d}\bar{x}} = \lambda^2\frac{A}{\bar{R}} - \mathrm{i}\frac{\bar{R}}{\lambda\bar{c}}J_{3D}, \tag{95}$$

and substituting (54) and (94) into (95) yields the amplitude equation for the oblique waves

$$\frac{\mathrm{d}A}{\mathrm{d}\bar{x}} = \kappa_{0b}A + \frac{3\pi}{10}\frac{\bar{R}^3}{\lambda}\mathrm{i}A^*A_0 + \mathrm{i}MA(\bar{x})\int_0^\infty |A(\bar{x}-x)|^2\,\mathrm{d}x, \tag{96}$$

where

$$\kappa_{0b} = \frac{4}{5}\left(\frac{\lambda^2}{2\bar{R}} - \tfrac{1}{8}\pi\frac{\bar{R}^2}{\lambda^3}\right), \tag{97}$$

and

$$M = -\frac{\pi}{5.6^{\frac{2}{3}}}\Gamma(\tfrac{1}{3})\,\bar{R}^4\sin^2\theta\tan^2\theta\cos 2\theta. \tag{98}$$

The first term in (96) characterizes the linear growth. The second term describes the fundamental–subharmonic mutual interaction that is termed, here, the parametric-resonance term. The third term describes the cubic, self-interaction of the oblique waves, which arises from the diffusion layer. Brown *et al.* (1993), in the context of Rayleigh wave–vortex interaction, have also obtained a nonlinear interaction term of the type given by the third term in (96). Wu *et al.* (1993) have shown that a term of this form arises in the very viscous limit of the original oblique mode analysis of Goldstein & Choi (1989).

For the plane wave we rewrite (16) as

$$\frac{\mathrm{d}A_0}{\mathrm{d}\bar{x}} = \frac{\lambda^2}{2^{\frac{3}{2}}\bar{R}}A_0 - \mathrm{i}\frac{\bar{R}}{\lambda\bar{c}}J_{2D}, \tag{99}$$

and substituting (57) into (99), yields the plane-wave amplitude equation which can be written as

$$\frac{\mathrm{d}A_0}{\mathrm{d}\bar{x}} = \kappa_0 A_0. \tag{100}$$

and shows that the plane wave follows the linear theory. The linear growth rate is given by

$$\kappa_0 = \frac{\lambda^2}{2^{\frac{3}{2}}\bar{R}} - \tfrac{1}{8}\pi\frac{\bar{R}^2}{\lambda^3}. \tag{101}$$

Equating κ_0 to zero gives Reid's (1965) equation (3.128) for the upper branch of the plane-wave neutral stability curve. The viscous Stokes layer contribution to the linear growth rate of the oblique waves in (97) is consistent with Smith & Stewart's (1987) result. Setting both of the linear growth rates in (97) and (101) to zero shows that the subharmonic oblique waves with $\theta = 60°$ and the plane fundamental wave reach their linear upper-branch neutral stability curves at $\bar{R}_{up,f} = 0.1537$ and $\bar{R}_{up,s} = 0.1725$, respectively. Equation (96) for the oblique waves along with (100) for the plane wave represent the final spatial evolutions for the resonant triad waves.

6. Nonlinear mechanisms for the triad's waves

We now examine the simultaneous development of the plane and oblique waves with the Reynolds number frozen in order to elucidate the role of the nonlinear mechanisms independently of the mean flow-divergence effects. The solution of the evolution equations, (96) and (100), is determined by the following initial conditions: the magnitude $|A_i|$ of the oblique wave amplitude; the magnitude $|A_{0i}|$ of the plane wave; the phase ψ_{0i} of the plane wave; and the initial phase of the oblique wave ψ_i, which is taken to be zero. The obliqueness angle is $\theta = 60°$. We first discuss in §6.1 the parametric resonance mechanism with the self-interaction between the oblique waves neglected. The effect of the self-interaction mechanism is then considered in §6.2.

6.1. *The parametric resonance mechanism*

We consider here the solution of the amplitude equations with the self-interaction term neglected. Perfect tuning is assumed herein; and the reader is referred to Mankbadi (1991*a*) for the effect of detuning. The evolution equations can then be solved analytically (for a frozen Reynolds number) to obtain

$$|A| = A_i \exp(\kappa_{0i}\bar{x}) \exp\left\{\frac{D}{\kappa_0}|A_{0i}|P + \tfrac{1}{2}\ln\left[\frac{1+c_4\exp[-4(D/\kappa_0)|A_{0i}|P]}{1+c_4}\right]\right\}, \tag{102}$$

where

$$P = \mathrm{e}^{K_0\bar{x}}, \quad D = \frac{3\pi}{10}\frac{\bar{R}^3}{\lambda}, \tag{103}$$

and the effective phase angle ψ_e defined as

$$\psi_e = \psi_0 - 2\psi, \tag{104}$$

is given by

$$\sin(\psi_e) = (r-1)/(r+1), \tag{105}$$

where

$$r = c_4\exp[-4(D/\kappa_0)|A_{0i}|P]. \tag{106}$$

The constant c_4 can be related to the initial phase angle ψ_{ei} by

$$c_4 = (1+\sin\psi_{ei})/(1-\sin\psi_{ei}). \tag{107}$$

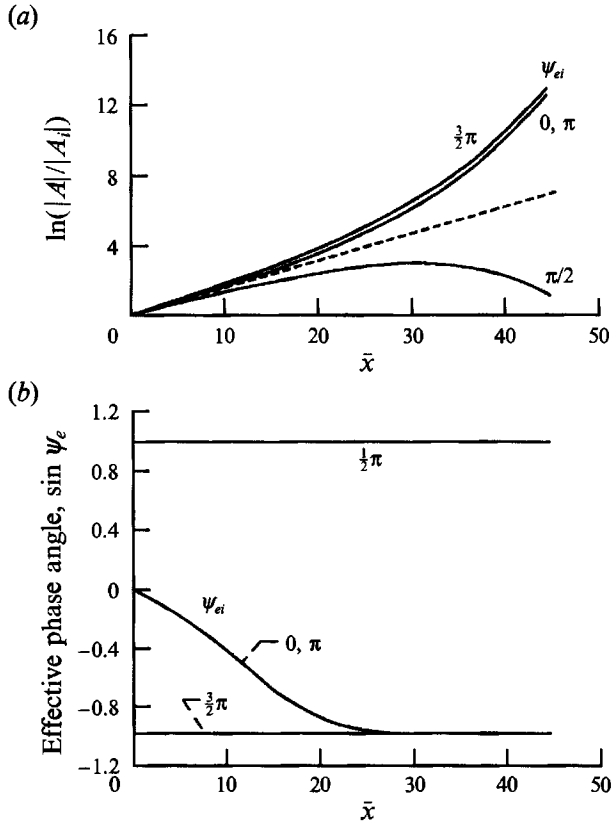

FIGURE 3. Development of the oblique waves at various initial phase-difference angles, ψ_{ei}, in the absence of the self-interaction mechanism. $A_{0i} = 2$, $R/R_{up,f} = 0.9$; ——, linear growth. (*a*) Magnitude; (*b*) phase.

The first exponential factor in (102) is the linear growth rate. The next exponential factor represents augmentation or suppression of the growth rate above the linear growth, depending on the initial phase angle ψ_{ei} (which determines c_4). Note that c_4 ranges from 0 to ∞. Two values of ψ_{ei} are of particular interest, $\psi_{ei} = \frac{1}{2}\pi$ and $\frac{3}{2}\pi$ (corresponding to $c_4 = \infty$ and 0, respectively). In either case (102) reduces to

$$|A| = |A_i| \exp(\kappa_{0b}\bar{x}) \exp(\pm(D/\kappa_0)|A_{0i}| \exp[\kappa_0 \bar{x}]), \tag{108}$$

with the negative sign in the second exponential factor corresponding to $\frac{1}{2}\pi$ and the positive sign corresponding to $\frac{3}{2}\pi$.

Figure 3 shows that the oblique waves initially exhibit a linear growth. This is followed by the parametric-resonance stage in which, exept for $\psi_{ei} = \frac{1}{2}\pi$, the presence of the plane wave causes a double-exponential growth given by the second exponential factor in (102).

6.2. *The self-interaction mechanism*

We now consider the solution of the evolution equations with the self-interaction term present. In figure 4 the initial phase difference angle is $\frac{3}{2}\pi$. In the parametric resonance stage the phase angle of the oblique waves for $\psi_{ei} = \frac{3}{2}\pi$ remains at its initial value. Because the coefficient of the self-interaction term is imaginary in (96), it causes an

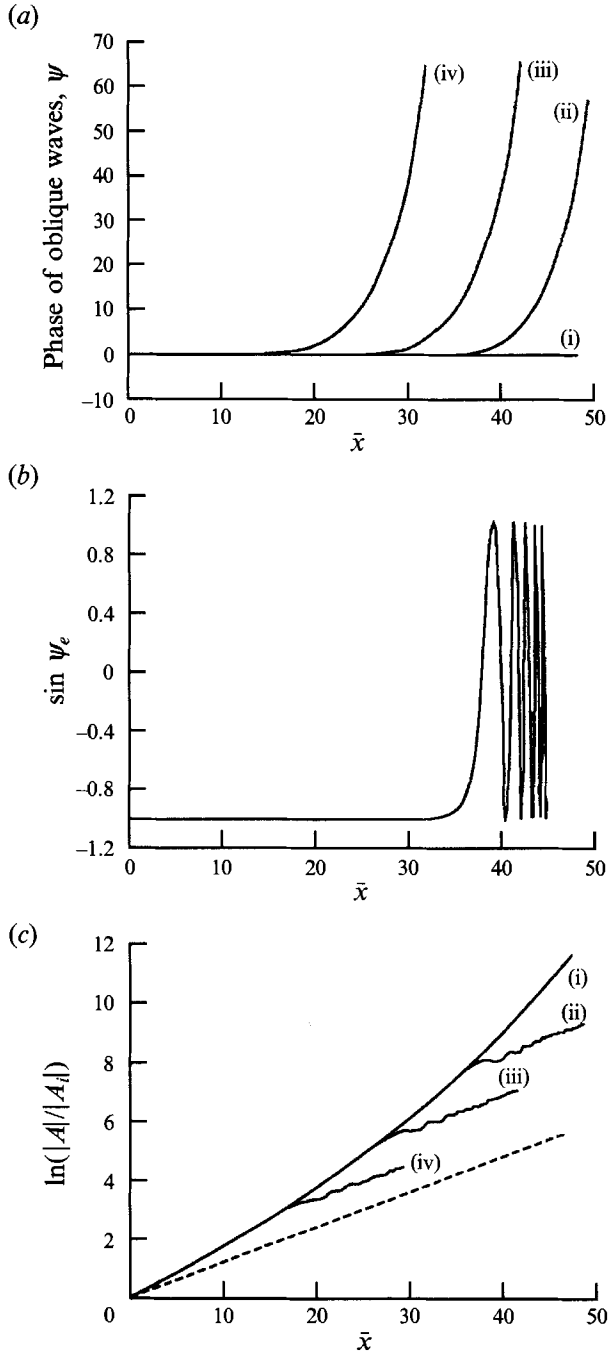

FIGURE 4. Effect of the self-interaction mechanism. $\psi_{ei} = 3\pi/2$, $A_{0i} = 5$, and $R/R_{up,f} = 0.95$. (*a*) Phase of oblique waves, (*b*) $\sin\psi_e$ for $A_i = 0.01$, (*c*) amplitude of oblique waves. (i) Parametric resonance with self-interaction term set to zero; (ii)–(iv) self-interaction accounted for: (ii) $A_i = 0.01$, (iii) $A_i = 0.1$, (iv) $A_i = 1.0$; ------, linear growth.

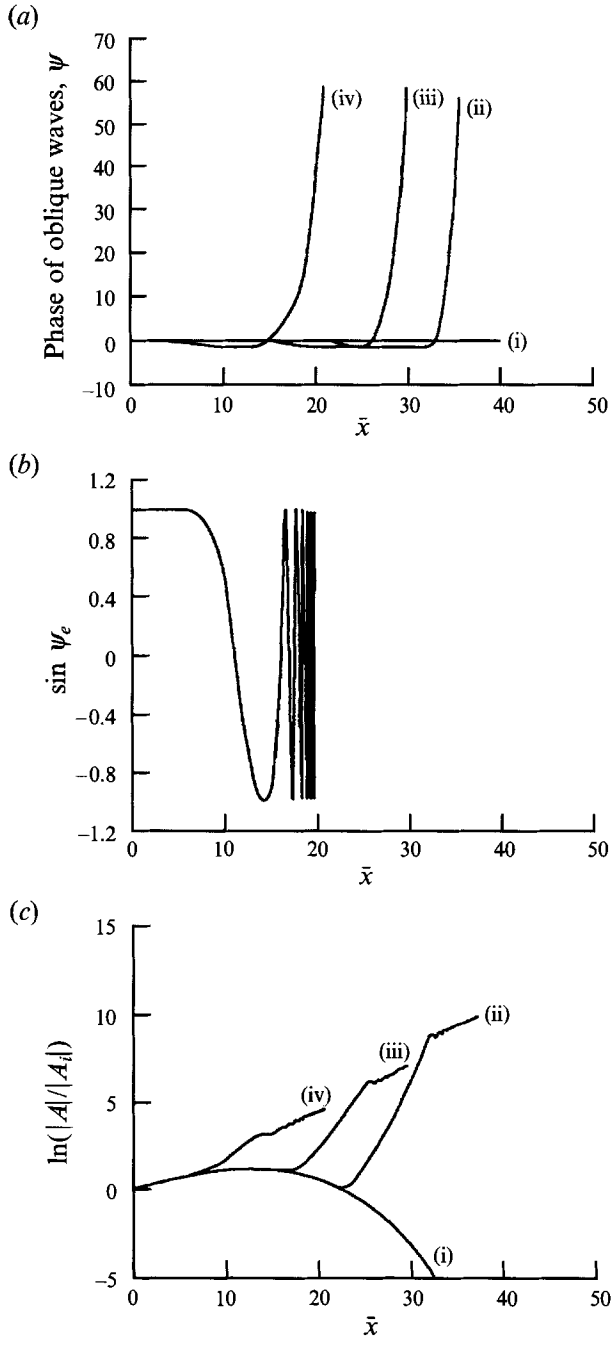

FIGURE 5. Effect of the self-interaction mechanism. $\psi_{ei} = \frac{1}{2}\pi$, $A_{0i} = 5$, and $R/R_{up,f} = 0.95$. (*a*) Phase of oblique waves, (*b*) $\sin\psi_e$ for $A_i = 1.0$, (*c*) amplitude of oblique waves. (i) Parametric resonance with self-interaction term set to zero. (ii)–(iv) self-interaction accounted for: (ii) $A_i = 0.01$, (iii) $A_i = 0.1$, (iv) $A_i = 1.0$.

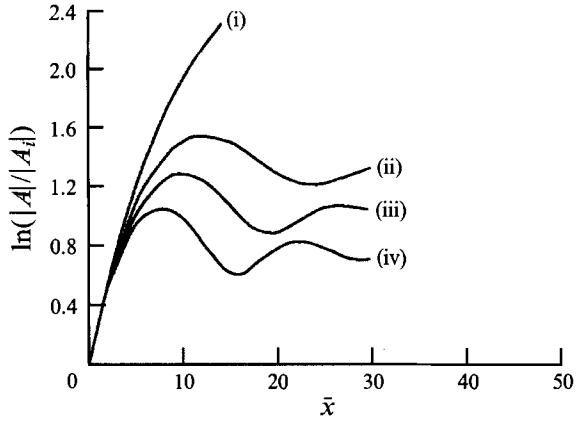

FIGURE 6. Effect of the self-interaction mechanism for zero linear growth of the oblique waves ($R = R_{up,s}$). $\psi_{ei} = \frac{3}{2}\pi$, $A_{0i} = 20$, (i) parametric resonance with self-interaction neglected, (ii)–(iv) self-interaction accounted for, A_i: (ii) 0.020, (iii) 0.022, (iv) 0.024.

explosive growth in the phase of the oblique waves (figure 4*a*). This introduces a rapid oscillations in $\sin\psi_e$ (see figure 4*b*), which determines the sign of the plane-oblique waves interaction term. Figure 4(*c*) shows that this effect causes oscillations in the amplitude to follow the parametric resonance stage. The increasingly rapid oscillations in $\sin\psi_e$ ultimately reduce the parametric resonance growth rate to oscillations around the linear growth rate. The results of figure 4 are repeated in figure 5 for an initial phase difference angle of $\psi_{ei} = \frac{1}{2}\pi$ wherein the parametric interaction initially suppresses the growth of the oblique waves. However, the figure indicates that the oblique waves self-interaction ultimately causes the same effect as that shown in figure 4.

The resonance phenomenon has always been found to occur in the vicinity of the upper branch where the linear growth rate is almost zero. The effect of self-interaction is shown in figure 6 for $R/R_{up,s} = 1$, i.e. for zero linear growth rate for the oblique waves. Under these conditions, the figure shows that the self-interaction causes the parametric resonance growth rate to be reduced ultimately to oscillations around the zero linear growth rate. This means that the self-interaction leads to oscillatory saturation, which may explain the observed saturation of the oblique waves. Self-interaction of a pair of oblique waves was first analysed by Goldstein & Choi (1989) for a free shear layer and was also found by Goldstein & Lee (1992) to play an important role in adverse-pressure-gradient boundary layers.

7. Discussion

In the pioneering work of Craik (1971) and its extension by Usher & Craik (1975), the coefficients in their equations for the temporally growing resonant triad were obtained using Stuart–Watson–Landau theory, which is not based on critical-layer nonlinearity. Their study suggested that the dominant contribution to the coefficients comes from the critical layer. In the present theory, which is for spatial growth, the amplitude equations are obtained by systematically considering the nonlinear/viscous critical-layer flow. This is consistent with Craik's earlier finding about the critical-layer contribution and leads to a truncated system that accounts for the additional modes generated by the nonlinear interactions in the critical layer. The present finding that the quadratic backreaction term is absent from the plane wave equation accords with

Usher & Craik's estimate that this term is smaller by a factor of R than the parametric resonance term in the oblique-waves equation. Also, the significant, cubic self-interaction of oblique waves, obtained here in a rigorous fashion, confirms Usher & Craik's estimate that large cubic interaction coefficients may be expected.

Smith & Stewart (1987) developed an asymptotic analysis of the resonant-triad interaction based on the triple-deck equations. Their results are focused on the case where nonlinearity comes into play at the Reynolds number and frequency range close to the lower branch, where the critical layer merges into the wall layer (lower deck) and its role was not considered in their analysis. This produces two-way coupling of oblique and plane waves as soon as the oblique waves become of the same order of magnitude as the plane wave. The present work differs from the triple-deck analysis of Smith & Stewart in several respects, the most important of which are: (i) the self-interaction of oblique waves is absent in the Smith & Stewart's (1987) analysis. The present work captures this self-interaction mechanism by allowing the oblique waves to grow from less-than to larger-than the plane wave. This mechanism turns out to be the significant mechanism in the nonlinear stage and it causes the experimentally observed saturation of the oblique waves. (ii) The linear and the fundamental-subharmonic interaction terms in Smith & Stewart have different numerical values from the present ones. This is not due to scaling of the amplitude functions, but results from the fact that Smith & Stewart's triple-deck analysis is concerned with modes relatively close to the lower branch. In contrast, the present analysis, in which the critical layer contribution is the key issue, is relevant to the streamwise region downstream of the lower branch.

Because, as the present analysis indicates, backreaction on the plane wave does not come into play in the parametric-resonance stage of interaction, this stage can be described by the linear secondary stability analysis of Herbert (1988), which assumes at the outset that the plane wave will continue to follow the linear theory. However, the next stage obtained here cannot be described by a secondary stability analysis, since this stage involves the self-interaction of the oblique waves.

Goldstein & Lee (1992) developed a first-principles, critical-layer theory for the nonlinear resonant triad in adverse-pressure-gradient boundary layers. The linear instability modes are inviscid, Rayleigh waves, as opposed to the viscous, Tollmien–Schlichting waves considered here. Their critical layer is growth-dominated, which leads to integro-differential equations for the amplitudes in which the backreaction of the oblique waves on the plane wave come into effect at a leading order. In the present analysis the backreaction is found to occur at higher-orders. The subharmonic self-interaction mechanism was significant in adverse-pressure-gradient boundary layers, as it is in the present Blasius boundary-layer case. However, because the Goldstein & Lee (1992) critical layer is non-equilibrium type, the self-interaction is in the form of a double integral and ultimately leads to explosive growth of the instability waves at a finite downstream position. In the present analysis it is possible to split the evolution equations as real equations for the magnitude and phase with the self-interaction terms appearing only in the phase equation. This causes an explosive growth in the phase of the oblique waves which causes the parametric resonance term to alternate signs. The net growth rate oscillates around the linear growth rate. Since the latter is almost zero in the nonlinear regime, the ultimate effect of the self-interaction mechanism is to produce saturation of the oblique waves, which will be discussed in greater details in a subsequent paper.

R.R.M. wishes to express his thanks to Dr M. E. Goldstein, who has specially influenced and inspired this work.

REFERENCES

BENNEY, D. J. & BERGERON, R. F. 1969 A new class of nonlinear waves in parallel flows. *Stud. Appl. Maths* **48**, 181–204.

BODONYI, R. J. & SMITH, F. T. 1981 The upper branch stability of the Blasius boundary layer, including non-parallel flow effects. *Proc. R. Soc. Lond.* A **375**, 65–92.

BROWN, P., BROWN, S. N. & SMITH, F. T. 1993 (In preparation).

CORKE, T. C. & MANGANO, R. A. 1989 Resonant growth of three-dimensional modes in transitioning Blasius boundary layers. *J. Fluid Mech.* **209**, 93–150.

CRAIK, A. D. D. 1971 Non-linear resonant instability in boundary layers. *J. Fluid Mech.* **50**, 393–413.

CRAIK, A. D. D. 1985 *Wave Interactions and Fluid Flow*. Cambridge University Press.

DRAZIN, P. G. & REID, W. H. 1981 *Hydrodynamic Stability*. Cambridge University Press.

GOLDSTEIN, M. E. & CHOI, W. W. 1989 Nonlinear evolution of interacting oblique waves on two-dimensional shear layers. *J. Fluid Mech.* **207**, 97–120. (See also Corrigendum, *J. Fluid Mech.* **216**, 659–663.)

GOLDSTEIN, M. E. & DURBIN, P. A. 1986 Nonlinear critical layers eliminate the upper branch of spatially growing Tollmien–Schlichting waves. *Phys. Fluids* **29**, 2344–2345.

GOLDSTEIN, M. E., DURBIN, P. A. & LEIB, S. J. 1987 Roll-up of vorticity in adverse-pressure gradient boundary layers. *J. Fluid Mech.* **183**, 325–342.

GOLDSTEIN, M. E. & LEIB, S. J. 1988 Nonlinear roll-up of externally excited free shear layers. *J. Fluid Mech.* **191**, 481–515.

GOLDSTEIN, M. E. & LEE, S. S. 1992 Fully coupled resonant-triad interaction in an adverse-pressure-gradient boundary layer. *J. Fluid Mech.* **245**, 523–551.

HALL, P. & SMITH, F. T. 1991 On strongly nonlinear vortex/wave interactions in boundary-layer transition. *J. Fluid Mech.* **227**, 641.

HERBERT, T. 1983 Subharmonic three-dimensional disturbances in unstable plane shear flows. *AIAA Paper* 83-1759.

HERBERT, T. 1988 Secondary instability of boundary layers. *Ann. Rev. Fluid Mech.* **20**, 487–526.

KACHANOV, YU. S. 1984 Development of spatial wave packets in boundary layer. In *Laminar–Turbulent Transition* (ed. V. V. Kozlov), Proc. Second IUTAM Symp. Novosibirsk, pp. 115–123. Springer.

KACHANOV, YU. S., KOZLOV, V. V. & LEVCHENKO, V. YA. 1978 Nonlinear development of a wave in a boundary layer. *Fluid Dyn.* **12**, 383–390.

KACHANOV, YU. S. & LEVCHENKO, V. YA. 1984 The resonant interaction of disturbances at laminar–turbulent transition in a boundary layer. *J. Fluid Mech.* **138**, 209–247.

KLEBANOFF, P. S., TIDSTROM, K. D. & SARGENT, L. M. 1962 The three-dimensional nature of boundary-layer instability. *J. Fluid Mech.* **12**, 1–34.

KLEISER, L. & ZANG, T. A. 1991 Numerical simulation of transition in wall-bounded shear flows. *Ann. Rev. Fluid Mech.* **23**, 495–537.

KNAPP, C. F. & ROACHE, P. J. 1968 A combined visual and hot wire anemometer investigation of boundary-layer transition. *AIAA J.* **6**, 29–36.

LIN, C. C. 1955 *The Theory of Hydrodynamic Stability*. Cambridge University Press.

LIN, C. C. 1957 On the instability of laminar flow and transition to turbulence. *IUTAM Symposium Freiburg/BR*, p. 144.

MANKBADI, R. R. 1990 Critical-layer nonlinearity in the resonance growth of three-dimensional waves in boundary layer. *NASA* TM-103639.

MANKBADI, R. R. 1991*a* Detuned triad interaction in boundary-layer instability. *Bull. Am. Phys. Soc.* JD6, **36**, 2713.

MANKBADI, R. R. 1991*b* Subharmonic route to boundary-layer transition: critical-layer non-linearity. In *Forum on Turbulent Flows* (ed. M. J. Morris *et al.*), ASME FED, vol. 112, pp. 75–81.

MANKBADI, R. R. 1993 The nonlinear interaction of frequency-detuned modes in boundary-layer transition. *AIAA*-93-0341.

MASLOWE, S. A. 1986 Critical layers in shear flows. *Ann. Rev. Fluid Mech.* **18**, 405–432.

RAETZ, G. S. 1959 A new theory of the cause of transition in fluid flows. Northrop Corp. Rep. NOR-59-383, Hawthorne, California.

REID, W. H. 1965 The stability of parallel flows. In *Basic Developments in Fluid Dynamics* (ed. M. Holt), pp. 249–308. Academic.

SARIC, W. S., KOZLOV, V. V. & LEVCHENKO, V. YA. 1984 Forced and unforced subharmonic resonance in boundary layer transition. *AIAA Paper* 84-0007.

SMITH, F. T. & STEWART, P. A. 1987 The resonant-triad nonlinear interaction in boundary-layer transition. *J. Fluid Mech.* **179**, 227–252.

USHER, J. R. & CRAIK, A. D. D. 1975 Nonlinear wave interactions in shear flows. Part 2. Third-order theory. *J. Fluid Mech.* **70**, 437–461.

WU, X. 1992 The nonlinear evolution of high-frequency resonant-triad waves in an oscillatory Stokes layer at high Reynolds number. *J. Fluid Mech.* **245**, 553–597.

WU, X. 1993 On the critical-layer and diffusion-layer nonlinearity in the three-dimensional stability of boundary layer transition. *Proc. R. Soc. Lond.* (to appear).

WU, X., LEE, S. S. & COWLEY, S. J. 1993 On the weakly nonlinear three-dimensional instability of shear layers to pairs of oblique waves: the Stokes layer as a paradigm. *J. Fluid Mech.* **253**, 681–721.